Acoustic Damage Localization for Suspension Bridge Main Cables

Tyler Pickering, Rebecca Cressman, Dylan Morano, Michael Smith, Daniel Baima

Professors Hu, Vincent

Friday 5$^{\text{th}}$ December, 2014

Contents

List of Figures

Chapter 1

Introduction

Modern day transportation relies heavily on large scale infrastructures such as: bridges, tunnels and overpasses. In particular, bridges serve to connect civilizations and provide a vital infrastructure. Because of this, it is important to maintain a high level of safety and these structures require careful maintenance and monitoring. The term structural health monitoring (SHM) refers to the process of implementing damage monitoring and a strategy of mitigating damage to engineering structures.

In the case of suspension bridges, the addition of cables under tension makes monitoring the structure a unique process. In general, suspension bridges, when properly cared for, have long service lives. The main cables used to support the hanger cables are composed of bundles, which are wrapped in soft wire and painted for protection. The wires are also galvanized, and when combined with the wrapping, offer good protection from the elements (Pure Technologies #). However, as mentioned by Higgens in his report, a well-documented vulnerability has manifested itself on several bridges in the United States: corrosion of main cables (Pure Technologies). Corrosion in the main cables is the primary reason for cables failing and snapping in the main bundle. When enough cable snaps occur, the loading capabilities of the bridge can be compromised. Proper monitoring of the bridges and their cables can help to keep the bridge in operation over large periods of time. However, this is a costly and labor intensive process.

According to a report by Pure Technologies on the Bear mountain Bridge A current visual inspection method[s] of a 10ft length of cable, wedging down 5 inches at 8 points around the circumference, only exposes one side of 4000 linear feet of weave, or 0.007% of the total length (Pure Technologies #). It should be noted that this method requires an observer, to visually inspect the wire. It was found that using this method to expose, inspect, and reinstate the cables costs on the order of $2 million dollars for 320ft (Pure Technologies #).

Newer methods for autonomous to semiautonomous monitoring would be beneficial in reducing the cost and labor involved in detecting these cable snaps. Using sensors to detect when and where cables snaps occurred could provide rapid health assessments of the structure, allowing mitigation steps to be taken. One possible method is to use acoustic monitoring sensors.

Acoustic monitoring has the potential to be able to detect breaks in suspension cables. Breaks in the cables create measurable acoustic events that passive systems can detect. In addition, active systems can inject signals into the bridge cables, having the sound travel the length of the wire. This method of monitoring holds the potential to greatly reduce or eliminate the need for cable inspection until a snap occurs. Furthermore, depending on package design, acoustic sensing could greatly reduce cost of operations.

1.1 Objectives

1.1.1 Phase one (Fall 2014)

The objective of the first phase of this study was to explore a methodology for determining the best frequencies of propagation on a suspension bridge main cable. A method was explored using the excitation of small-scale steel rods in order to be applied to large scale system. This was to involve the testing of theoretical calculations to determine whether or not resonant frequencies could be accurately predicted using the methods described in section (SITE THEORY SECTION HERE). Experiments were to be carried out on a small scale steel rod for several types of excitations. The results of which were to be compared to the expected theoretical calculation to verify the accuracy of the prediction methods. Resonant frequencies were selected to be the best frequencies of propagation due to the fact that they cary the best in a medium. Injection of a signal at the resonant frequency of a medium would require less amplitude than other spectra and might result in a stronger response of returned signal.

Chapter 2

Frequency Predictions

Frequency Analysis Modal analysis is the analytical evaluation of the modal shapes and natural frequencies a vibrating system assumes. Theoretical frequencies are calculated using modal analysis for predetermined modes. These theoretical results are compared with experimental results to determine accuracy. Both transverse and axial waves were used as vibration stumuli in this report. A transverse wave is a moving wave where the particle displacement motion oscillates perpendicular to the direction of propagation. Whereas an axial wave is a moving wave where the particle displacement oscillates parallel to the direction of wave propagation.

Wave Speed Any sinusoidally oscillating system governed by Equation 2.1, which is the second derivative of the progressive wave function Equation 2.2, with wavelength λ, will travel with speed v.

$$\frac{d^2y}{dx^2} = \frac{1}{c^2}\frac{d^2y}{dt^2} \tag{2.1}$$

$$y = A\sin\frac{2\pi}{\lambda}(x + ct) \tag{2.2}$$

For a solid rod, c is a function of Young's Modulus Y and the density ρ of the material, displayed in Equation 2.3.

$$c = \sqrt{\frac{Y}{\rho}} \tag{2.3}$$

Modal Frequency The modal frequencies in the axial direction were calculated using the methods described by Kinsler, Frey, Coppens, and Sanders in Fundamentals of Acoustics. The boundary conditions for a rod fixed at both ends were applied to the wave equation. After applying the boundary conditions the frequencies of the natural modes of vibration in the axial direction can be calculated using Equation 2.5.

$$y(x,t) = Ae^{j(\omega t - kx)} + Be^{j(\omega t - kx)} \tag{2.4}$$

By application of the boundary equations to the wave equation gives

$$f_n = \frac{n}{2}\frac{c}{L} \tag{2.5}$$

Where n corresponds to each fundamental mode, L is the length of the rod, and f_n is the fundamental frequency corresponding to each mode n. The modal frequencies of the natural modes of vibration in the transverse direction were calculated using Equation 2.6.

$$f_n = 0.441(n + 0.5)^2 f_1 \tag{2.6}$$

Where the frequency f_1 is governed by the speed of sound in the specific medium. This can be seen below in Equation 2.7.

$$f_1 = 1.028\frac{a}{L^2}\sqrt{c} \tag{2.7}$$

Where a is the thickness of the rod.

Chapter 3

Experiments

3.1 Free Hanging Resonance Tests with a PMNT Piezoelectric Sensor

Several experiments were carried out on a 20 foot long, 1/4th inch 114R steel rod. These tests were performed in order to determine the methodology for finding resonant frequencies of the rod when excited with both longitudinal (axial) and transverse (shear) waves. The purpose of these tests was to experimentally validate the described method for determining resonant frequencies in a free hanging metal rod. Tests were performed using multiple types of piezoelectric sensors as contact microphones for observing and analyzing the response of exciting vibrations along the rod.

3.1.1 Experimental Procedure

A steel rod was suspended from 4 equally spaced laboratory stools using elastic bands in order to isolate the vibrations from the rod to the stools. This method was used in order to attempt to represent an ideal free hanging rod with no support on either end. A PMNT piezoelectric sheet was attached around the rod at one of the free hanging ends and connected to a computers sound card using a 3.5mm patch cable. The attached piezoelectric sensor and rod can be seen below in Figure 3.1 as well as the elastic suspension of the rod in Figure 3.2.

Figure 3.1: Suspension of steel test bar

Figure 3.2: PMNT Sensor placement on end of bar

The rod was excited mechanically using the strike of a hammer and a rubber mallet. With the piezoelectric sensor secured around the end of the rod as seen above, the rod was struck at the opposing endpoint using both the mallet and the hammer. This was done in order to produce an axial (or longitudinal) wave propagation down the length of the rod. The produced sound data was recorded in to individual files. The rod was then struck on its midpoint in the same manor in order to generate a transverse wave. The data was recorded for each striking surface. This procedure yielded 4 sets of sound data. The sets corresponded to metal and rubber strikes for both longitudinal and transverse excitations along the rod with the sensor recording near the endpoint.

The sensor was then repositioned to the midpoint of the metal rod. Sound data was collected once again for transverse and longitudinal excitations. Once again the endpoint of the rod was struck longitudinally using both a hammer and rubber mallet to axially excite the rod. In order to excite the rod transversely, the rod was struck on its *side* very close to the end point. These strikes were recorded individually to produce 4 more sets of data. This data corresponded to metal and rubber strikes for both longitudinal and transverse excitations along the rod with the sensor recording at the midpoint.

3.1.2 Results and Analysis

The 8 data sets from the experiment were interpolated with MATLAB and cropped to the beginning of each strike. The cropped waveform for the axial rubber mallet strike, with the sensor recording from the opposite endpoint, can be seen below in Figure 3.3.

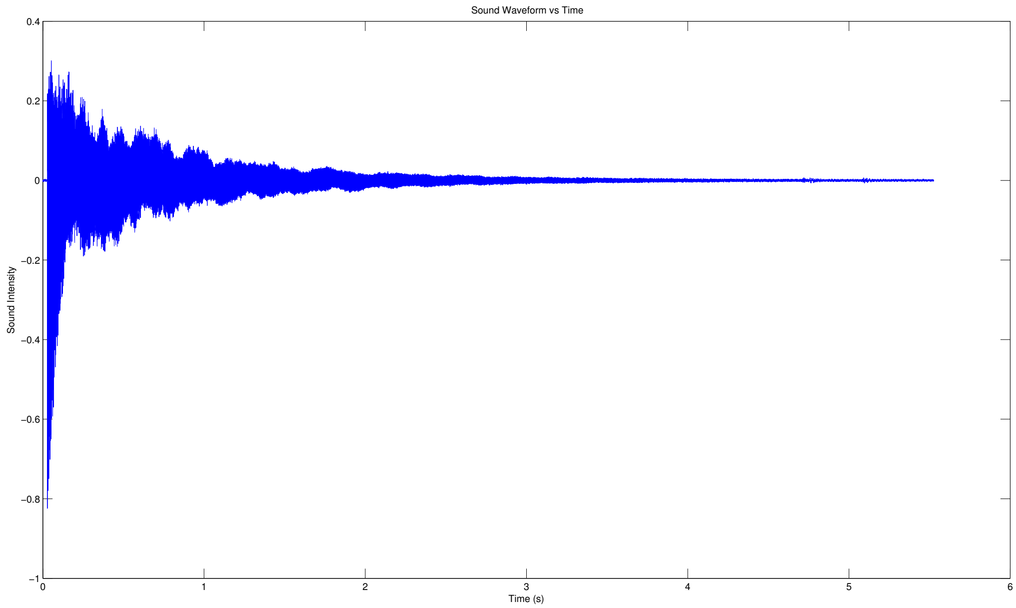

Figure 3.3: Waveform for cropped rubber mallet axial strike (sensor at opposing endpoint)

This is an example of the sound data produced for each strike during the experimental trials. Each one of these datasets was then analyzed for frequency content using the method of Fourier Analysis. The Fast Fourier Transform was taken for each dataset and the FFT of the above axial rubber strike can be seen below in Figure 3.4.

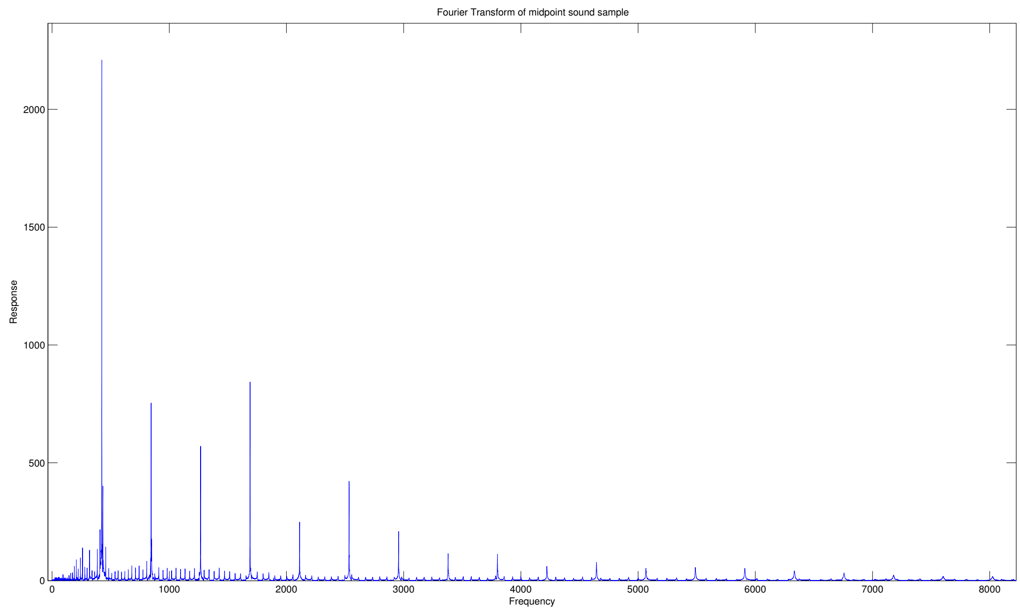

Figure 3.4: FFT for cropped rubber mallet axial strike (sensor at opposing endpoint)

Several definitive peaks can be seen steadily decreasing along the spectrum as frequency increases. These peaks correspond to the first several resonant modal frequencies of the free hanging rod in excitation. The first and strongest frequency response is seen to be at 424.8 Hz. This was repeated for each trial and the results were tabulated.

It was discovered during this analysis that several of the data sets were very noisy and it was nearly impossible to extract a pattern of frequencies. The trials which produced these results were both the transverse excitations with the sensor near the endpoint and the transverse excitation using the rubber mallet with the sensor at the midpoint. The only transversely excited dataset which produced a clean spectra was the metal hammer strike with the sensor at the midpoint. An FFT from one of these noisy data sets can be seen below in Figure 3.5.

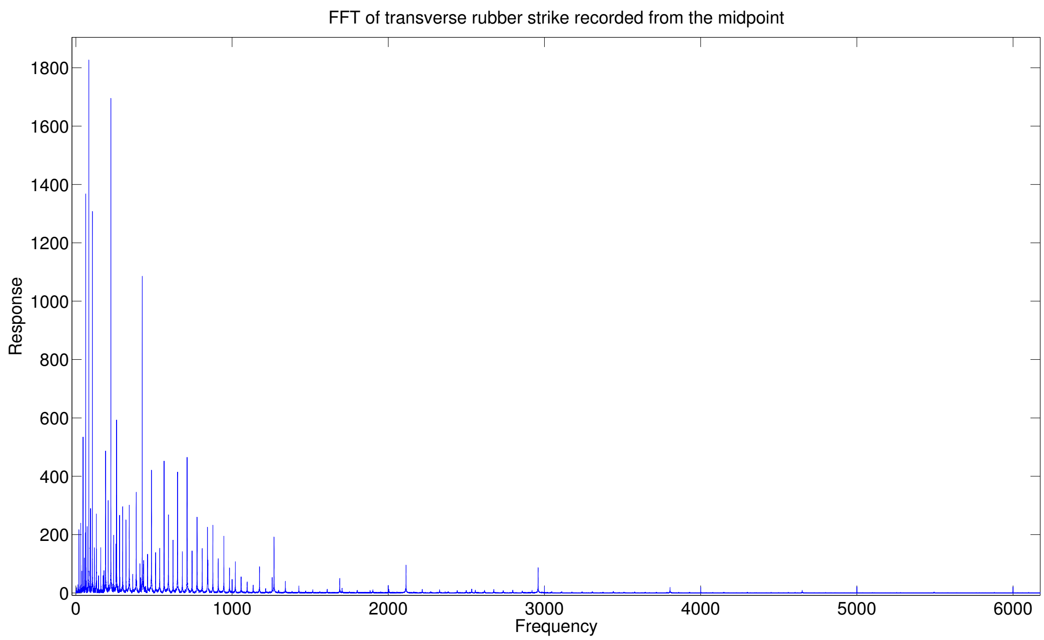

Figure 3.5: Noisy FFT data from transverse rubber mallet strike recorded at midpoint

This may have been as a result of attempting to measure axial vibrations from a transverse excitation, and a weak strike using the rubber mallet.

In the following tables, the first 8 discovered frequencies can be seen alongside the expected theoretical frequencies calculated in the previous section.

Dominant frequency	1	2	3	4	5	6	7	8
Axial midpoint Metal	424.8 Hz	845.9 Hz	1269 Hz	1691 Hz	2113 Hz	2535 Hz	2959 Hz	3379 Hz
Axial midpoint rubber	424.8 Hz	845.2 Hz	1269 Hz	1690 Hz	2114 Hz	2534 Hz	2960 Hz	3379 Hz
Axial endpoint metal	424.8 Hz	845.7 Hz	1269 Hz	1690 Hz	2114 Hz	2534 Hz	2960 Hz	3379 Hz
Axial endpoint rubber	424.8 Hz	845.5 Hz	1268 Hz	1690 Hz	2114 Hz	2534 Hz	2960 Hz	3379 Hz
Theoretically Expected	415.3 Hz	830.7 Hz	1245.98 Hz	1661.4 Hz	2076.7 Hz	2493 Hz	2907.3 Hz	3322.6 Hz

Table 3.1: FFT extracted frequencies for each trial compared to theoretically expected frequencies

3.2 Free Hanging Resonance Tests with a PZT Piezoelectric Sensor

Another series of experiments were carried out on the same steel rod as before. For these tests, a small circular (0.5cm) PZT sensor was used in place of the PMNT film. The PZT sensor was placed on the endpoint of the rod for these experiments. This was to assure that the PZT would be primarily measuring the rods axial responses to excitation. The PZT sensors were also placed on the side of the rod, however their brittleness caused them to shatter easily when this was attempted. Several experiments were carried out including a set of trials similar to the above section and a transverse ”pluck” test. For this test, the rod was deflected at its midpoint and released. The results from this ”pluck” were recorded with the PZT sensor at the end point to determine whether or not the transverse deflection would excite a measurable axial response.

Appendices

Appendix A

MATLAB Calculations